JMEPEG (2020) 29:1479–1487
https://doi.org/10.1007/s11665-019-04493-2

1059-9495/$19.00

Influence of Selected Deoxidizers on Chemical Composition of Molten Inclusions in Liquid Steel

Dorota Kalisz, Piotr Migas, Mirosław Karbowniczek, Michał Moskal, and Andrzej Hornik

(Submitted August 27, 2019; in revised form November 6, 2019; published online December 9, 2019)

The conditions of nonmetallic inclusions formation by using manganese, silicon, and aluminum deoxidizers in a steel bath (four steel grades) are reviewed in the presented paper. The changes in the chemical composition of nonmetallic inclusions were calculated under thermodynamic equilibrium conditions between liquid steel containing Mn, Si, O, Al and the formed liquid oxide phase, applying a non-commercial (author's) computer program. The impact of the order of dispensing alloy additions, and the initial manganese content in steel on the final oxygen concentration, as well as the evolution of the chemical composition of nonmetallic inclusions were considered. The acquired results indicate that the proposed calculation procedure can be used to design the desired chemical composition of steel with a controlled value and chemical composition of nonmetallic inclusions.

Keywords deoxidation, nonmetallic inclusions, steel processing, thermodynamic calculations

1. Introduction

Nonmetallic inclusions in steel lower its mechanical properties, and their presence also causes several problems during metal forming (Ref 1). Inclusions act as places of crack initiation, in particular if products are subjected to cyclic loading (Ref 1-4). Thus, the presence of nonmetallic inclusions is particularly harmful, e.g., in spring steels or automotive steels. Note that the formation of nonmetallic inclusions is strictly related to deoxidizing processes and no steel manufactured is fully free of nonmetallic phase inclusions (Ref 5-9). Commonly used deoxidisers are Si, Mn and Al (and these elements occur in the steel chemical composition), and hence one should pay special attention to the phase diagram MnO-SiO_2-Al_2O_3 (Ref 10-12). Research on the evolution of nonmetallic inclusions in steels deoxidised with Mn and Si has confirmed that nonmetallic inclusions of type MnO-SiO_2-Al_2O_3 have a low melting temperature and therefore easily deform during rolling.

Knowledge of activities of liquid oxide phase constituents is based upon experimental data, and the curve of variability of activity in binary solutions, as well as changes caused by temperature, are not well enough described in the literature (Ref 13-16).

The control of the amount and chemical composition of nonmetallic inclusions, in particular to eliminate larger inclusions, is a process of elementary significance for the quality of the steel manufactured. The foundation for the analysis of the behavior of precipitates in liquid steel is the determination of their quantity and chemical composition, which can be done, e.g., by using chemical analysis, x-ray microanalysis and thermodynamic calculations. The chemical composition of the formation of nonmetallic inclusions can be determined, when knowing the concentrations of O, Mn, Si and Al in steel. The objective of the presented study was to determine the quantity of oxide nonmetallic inclusions present in a ladle as a result of dosing deoxidisers into the ladle in the conditions of thermodynamic equilibrium with reference to the actual process, using the authors' original IT tools.

2. Description of Thermodynamic Equilibrium in the Liquid Steel-Oxide Phase System

The calculations in the study included chemical composition and the amount of two liquid phases staying in the state of thermodynamic equilibrium: steel and a solution of the selected oxides. The analysis was limited to the most important components: iron, manganese, silicon, aluminum, oxygen and carbon. The equilibrium between the phases at a specific temperature is set by oxidation reactions (Ref 12, 13, 17):

$$Mn + O = MnO \quad \text{(Eq 1)}$$

$$Si + 2O = SiO_2 \quad \text{(Eq 2)}$$

$$2Al + 3O = Al_2O_3 \quad \text{(Eq 3)}$$

On the basis of the literature (Ref 13, 15, 16), it was found that at the temperatures assumed for the computing, liquid nonmetallic inclusions could precipitate from the system: MnO-SiO_2-Al_2O_3, and they could form a solution. Therefore, it is

This article is an invited submission to JMEP selected from presentations at The XXII Physical Metallurgy and Materials Science Conference: Advanced Materials and Technologies (AMT 2019) held June 9-12, 2019, in Bukowina Tatrzanska, Poland, and has been expanded from the original presentation.

Dorota Kalisz, Piotr Migas, and **Mirosław Karbowniczek**, AGH-University of Science and Technology, 30 A. Mickiewicza Av., Kraków, Poland; **Michał Moskal** and **Andrzej Hornik**, COGNOR SA Branch HSJ in Stalowa Wola, Kwiatkowskiego 1, Stalowa Wola, Poland. Contact e-mails: dak@agh.edu.pl, pmigas@agh.edu.pl, mkarbow@agh.edu.pl, and hsj@hsjsa.pl.

assumed that the products forming in the deoxidizing process are liquid. Equilibrium constants for these reactions, coupling the activities of components of both phases, are as follows (Ref 12, 13, 18):

$$K_{(\mathrm{MnO\ l})} = \frac{a_{\mathrm{MnO}}}{a_{\mathrm{Mn}} \cdot a_{\mathrm{O}}} = \frac{a_{\mathrm{MnO}}}{f_{\mathrm{Mn}} \cdot [\mathrm{Mn}] \cdot f_{\mathrm{O}} \cdot [\mathrm{O}]} \quad \text{(Eq 4a)}$$

$$\log K_{(\mathrm{MnO\ l})} = 11{,}749/T - 4.67 \quad \text{(Eq 4b)}$$

$$K_{(\mathrm{SiO_2\ l})} = \frac{a_{\mathrm{SiO_2}}}{a_{\mathrm{Si}} \cdot (a_{\mathrm{O}})^2} = \frac{a_{\mathrm{SiO_2}}}{f_{\mathrm{Si}} \cdot [\mathrm{Si}] \cdot (f_{\mathrm{O}})^2 \cdot [\mathrm{O}]^2} \quad \text{(Eq 5a)}$$

$$\log K_{(\mathrm{SiO_2\ l})} = 30{,}110/T - 11.40 \quad \text{(Eq 5b)}$$

$$K_{(\mathrm{Al_2O_3 l})} = \frac{a_{\mathrm{Al_2O_3}}}{(a_{\mathrm{Al}})^2 \cdot (a_{\mathrm{O}})^3} = \frac{a_{\mathrm{Al_2O_3}}}{(f_{\mathrm{Al}})^2 \cdot [\mathrm{Al}]^2 \cdot (f_{\mathrm{O}})^3 \cdot [\mathrm{O}]^3} \quad \text{(Eq 6a)}$$

$$\log K_{(\mathrm{Al_2O_3\ l})} = 64{,}000/T - 20.57 \quad \text{(Eq 6b)}$$

Activities of oxide phase components concern pure liquid oxides as a standard state. For activities of liquid steel components—the reference is a diluted solution, in which the activity according to Henry's law is equal ($a = f \cdot [\%i]$) to the concentration of component expressed in mass percentage. The relationships (4b), (5b) and (6b) come from the paper by Liu et al. (Ref 17). However, the oxidation of iron, causing the occurrence of iron oxides as components of the oxide phase, has not been taken into account. It arises from the dependence presented by Turkdogan (Ref 19):

$$\log \frac{[\%\mathrm{O}]}{(a_{\mathrm{FeO}})} = -\frac{6692}{T} + 3.03 \quad \text{(Eq 7)}$$

that for the temperature of 1873 K, at oxygen concentration in steel of 100 ppm or 10^{-2}% by mass, the activity of FeO will be ca. 2.9×10^{-3}. For this activity, the concentration X_{FeO} is below 0.01, and the formation of Fe_2O_3 is not possible. It is confirmed by experimental results of equilibrium compositions of steel and slag presented in the paper by Ohta and Suito (Ref 13), where concentrations of FeO in slag reached a few molar percent at a very low aluminum concentration in steel. Among the model assumptions, also the presence of carbon (e.g. in the form of carbonates), sulfides and oxisulfides in the nonmetallic phase was neglected.

Activity coefficients of liquid steel components are expressed with the equation of Wagner–Chipman (Ref 12).

$$\log f_i = e_i^{\mathrm{Mn}} \cdot [\%\mathrm{Mn}] + e_i^{\mathrm{Si}} \cdot [\%\mathrm{Si}] + e_i^{\mathrm{Al}} \cdot [\%\mathrm{Al}] + e_i^{\mathrm{O}} \cdot [\%\mathrm{O}] + e_i^{\mathrm{C}} \cdot [\%\mathrm{C}] \quad \text{(Eq 8)}$$

where i = Mn, Si, Al, O. The values of impact parameters e_i^j are adopted from the paper by Liu et al. (Ref 17) (Table 1).

Table 1: The values of impact parameters e_i^j in Eq 8 for the temperature 1873 K (Ref 12, 17)

The activities of constituents of the liquid oxide phase were determined for the model of regular solution (Ref 12, 20):

$$RT \cdot \ln \gamma_i = \sum_j \alpha_{ij} \cdot X_j^2 + \sum_j \sum_k \left(\alpha_{ij} + \alpha_{ik} - \alpha_{jk}\right) \cdot X_j \cdot X_k \quad \text{(Eq 9)}$$

The activities of constituents are referred to pure liquid constituents: MnO, SiO_2, $AlO_{1.5}$.

Taking into account the stoichiometry of all oxides analyzed in the model (as above), it is necessary to convert the activity of Al_2O_3 to $AlO_{1,5}$; therefore, the correlation between the activity of $AlO_{1.5}$, and the activity of Al_2O_3 was applied according to Eq 10:

$$a_{\mathrm{Al_2O_3}} = (a_{\mathrm{AlO_{1.5}}})^2 \quad \text{(Eq 10)}$$

The following values of parameters α in Eq 9 were assumed:

$\alpha_{\mathrm{MnO,SiO_2}} = -75{,}310$ (Ref 20) and $\alpha_{\mathrm{SiO_2,AlO_{1.5}}} = -87{,}000$ (Ref 21).

The chemical composition of liquid steel and nonmetallic inclusions in the equilibrium state is computed by solving a system of Eq 4a, 5a and 6a, where after making necessary substitutions, the concentrations of both phases are the variables. The concentrations for the oxide phase are expressed in molar fractions, and for steel in mass percentage. A computer program was used to solve this problem, and the details of its operation are described in papers (Ref 6, 7, 11, 12).

3. The Steel Subject to Analysis of Oxide Inclusion Formation

The value of thermodynamic affinity of metals to oxygen indicates that aluminum, silicon and manganese can be used as deoxidisers. These metals are introduced to the ladle to deoxidize and modify steel chemical composition. The refining effect, i.e., the degree of deoxidation and the obtained composition of steel and refining products (oxide precipitates), can be calculated on the basis of the thermodynamic equilibrium state, which forms between two phases: the diluted liquid solution of Mn, Si, Al in iron and the nonmetallic phase comprising MnO, SiO_2 and Al_2O_3. The process of deoxidation and formation of the nonmetallic phase was simulated for 4 types of steel, the chemical composition of which is presented in Table 2.

Table 1 The values of impact parameters e_i^j in Eq 8 for the temperature 1873 K (Ref 12, 17)

	j				
i	**Mn**	**Si**	**Al**	**O**	**C**
Mn	0	−0.0327	0.027	−0.087	−0.0538
Si	−0.0146	0.103	0.058	−0.119	0.18
Al	0.035	0.056	0.043	−1.98	0.091
O	−0.0224	−0.066	−1.17	−0.17	−0.42

Table 2 Chemical composition of steel (% by weight)

Steel	C	Mn	Si	Cr	Ni	Mo	S_{max}
1	0.16	1.20	0.20	0.90	1.40	0.25	0.02
2	0.18	0.70	0.20	1.60	1.50	0.30	0.02
3	0.42	0.70	0.20	1.10	0.20	0.20	0.02
4	0.16	1.0	0.20	0.90	0.30	0.08	0.02

A simplified model was used for computing, considering the equilibrium in a 7-component system: Fe, C, Mn, Si, Al, O, S, characteristic for the steels concerned, where the main chemical constituents are presented in Table 2.

Table 2: Chemical composition of steel (% by weight).

It was also assumed that Fe, C and S only occur in the metallic phase. If the deoxidizing products form a solution, then in the conditions of equilibrium, between the metallic and oxide phases, the actual values of deoxidizing product activities in this solution should be taken into account. A description of the thermodynamic equilibrium state requires knowledge of the temperature, pressure and mass of all components present in all phases in the system. The thermodynamic condition for the formation of any A_aB_b inclusion is exceeding the equilibrium value of solubility product Q (Ref 21).

$$Q_{\text{rzecz}} > Q \cdot a_{A_aB_b} \quad \text{(Eq 11)}$$

$a_{A_aB_b}$—thermodynamic activity of the compound A_aB_b

$$Q_{\text{rzecz}} = [[A]^a.[B]^b] \quad \text{(Eq 12)}$$

where a, b—stoichiometric coefficients, A, B—components taking part in the reaction.

4. Refining Procedure

The actual ladle refining process for the steels in question was simulated using the following assumptions: process time was 30 min, the initial mass of the nonmetallic phase—the primary slag— was 50 kg. (It was assumed that this was a residue after preliminary steel deoxidizing, i.e., after removing the primary slag from preliminary refining.)

The chemical composition of the sample taken from the primary ladle slag contained: 45% CaO, 2% Al_2O_3, 9% MgO, 5% MnO, 12% SiO_2, 27% FeO, the refining process temperature was 1620 °C (tapping temperature: 1600-1620 °C), the mass of steel in the ladle 45 Mg, the initial content of oxygen 0.01%, the sulfur content 0.005%. The following procedure of introducing the alloy additions: in the first step of the process, 30 kg of Mn was added in the form of (FeMn), in the second step 30 kg of Si in the form of FeSi, and in the third step 30 kg of Al.

5. Results of Simulations

For the set amounts of Mn, Si and Al fed to the steel, the influence of these additions on the oxygen content in the steel and the amount and chemical composition of the formed oxide phase was determined. Figure 1 and 2 presents the computing results for changes in the content of basic components of steel 1 as a result of dosing alloy additions, and the change in the chemical composition of nonmetallic inclusions. The following figures (Fig. 3, 4, 5, 6, 7, 8, 9) present the simulation results for steels Nos. 2, 3 and 4, with their chemical compositions presented in Table 2.

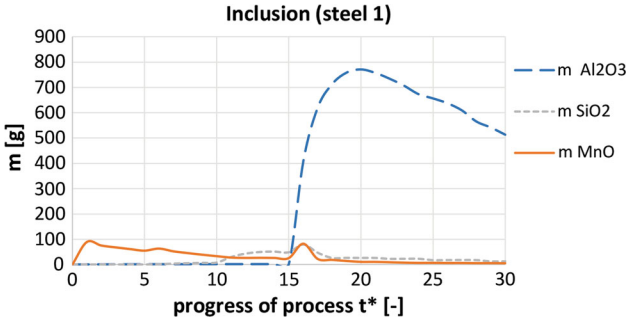

Fig. 2 Change in the chemical composition of nonmetallic inclusions as a result of dosing alloy additions to steel 1

Introduction of the primary slag with the above-specified composition to the system (model) influences the curve of variability of the oxygen concentration in steel during refining (Fig. 1b, 3b, 5b, and 7b). Thus, the oxygen concentration in steel is an effect of achieving the equilibrium state between the metallic and nonmetallic phases in the next computing step.

In the initial phase of the process, primarily the MnO oxide phase forms. The addition of FeSi results in the formation of the SiO_2 phase. An increased share of manganese oxide in inclusions is caused by the initial high content of Mn (1.2%). The introduction of Al in the final phase of refining causes precipitation of aluminum oxide, and in effect the oxygen content drops to 10 ppm, and the final composition of inclusions is dominated by the presence of Al_2O_3.

The calculations have established that the share of MnO oxide in inclusions increases up to 100 g already in the first step of the process (Fig. 4), and then it decreases to the level of about 15 g in the fifteenth minute, and then it increases by about 0.5 min up to 90 g, and decreases as a result of a change in the oxygen and manganese content in the solution. The continuation of the deoxidizing process and introducing subsequent deoxidizing additions results in the formation of phase SiO_2 and Al_2O_3 and restricts the formation of MnO.

For steel 2 (Fig. 3), as a result of dosing alloy additions, the final oxygen content in steel was obtained at a level of 11 ppm. When adding deoxidizing additions, the share of individual oxides changes, and the addition of aluminum results in the

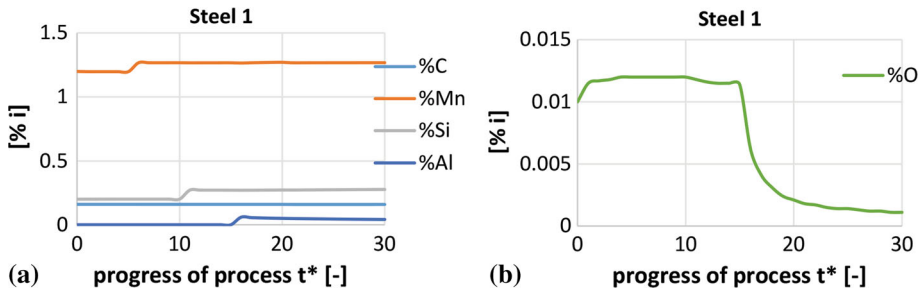

Fig. 1 Change in the chemical composition of steel (a) and (b) as a result of dosing alloy additions

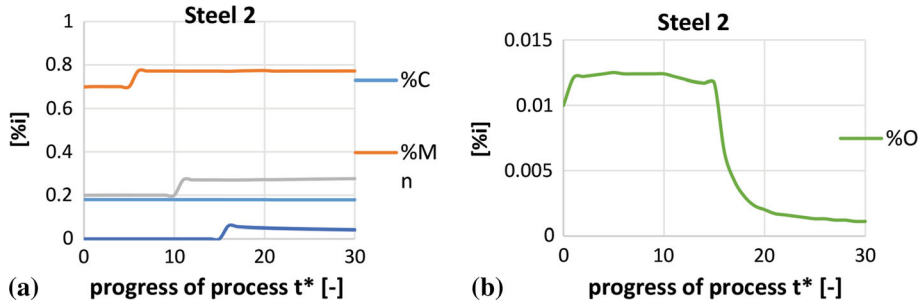

Fig. 3 Change in the chemical composition of steel 2 as a result of dosing alloy additions

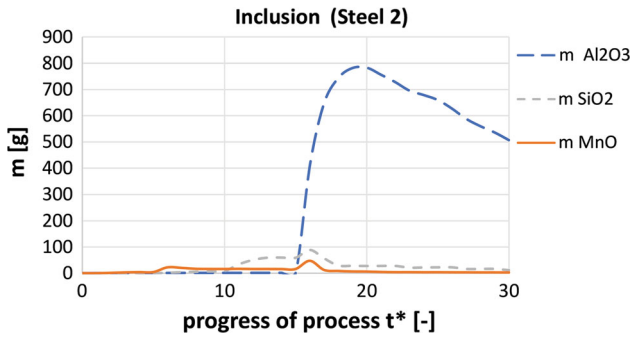

Fig. 4 Chemical composition of nonmetallic inclusions as a result of dosing alloy additions to steel 2

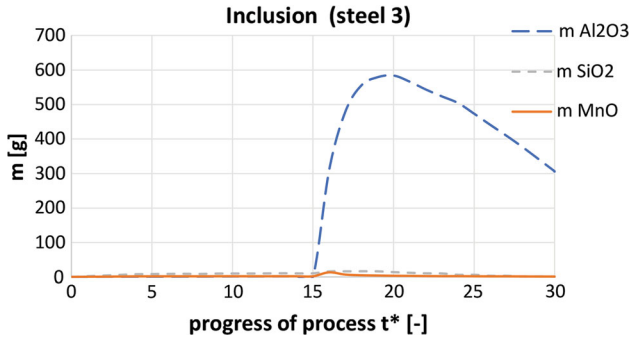

Fig. 6 Chemical composition of nonmetallic inclusions as a result of dosing alloy additions to steel 3

formation of aluminum oxide only in the final phase of the process.

For steel 3, the lowest final oxygen content in steel was obtained—5 ppm. When compared to steels 1 and 2, a lower share of SiO_2 and MnO in inclusions was found. Before feeding aluminum in the fifteenth minute of the process, the dissolved oxygen share was about 48 ppm, and, as a result of supplying aluminum to the system, the forming oxide phase consisted of over 90% Al_2O_3.

Figure 9 and 10 shows results of simulation for steel 4.

We can state that the influence of aluminum addition on its concentration in liquid steel is a consequence of deoxidizing and its majority goes to the nonmetallic phase. The impact of other deoxidisers, i.e., Mn and Si, is not decisive to the final concentration of Al in steel. The addition of Al causes a reduction in the final oxygen content in steel to very low values, even 2 ppm (computed—Fig. 9). The forming nonmetallic phase is treated as a liquid oxide solution. The addition of Mn and Si has a different impact on changes in the oxide content than the addition of Al. In the first phase of the process oxide MnO prevails, its amount is a consequence of introducing it as an addition and its initial share in the steel. The biggest amount of the forming MnO was observed in steels 1 and 2, where the initial Mn content in steel was 1.2 and 1%, respectively, and the final Mn concentration is determined by the standard for the steel grade produced. As a result of the Si introduction, complex inclusions MnO-SiO_2 form. For instance, when determining the deoxidizing capacity of a single deoxidiser, or a group of them, it was computed that if manganese was the only deoxidiser applied, at its concentration

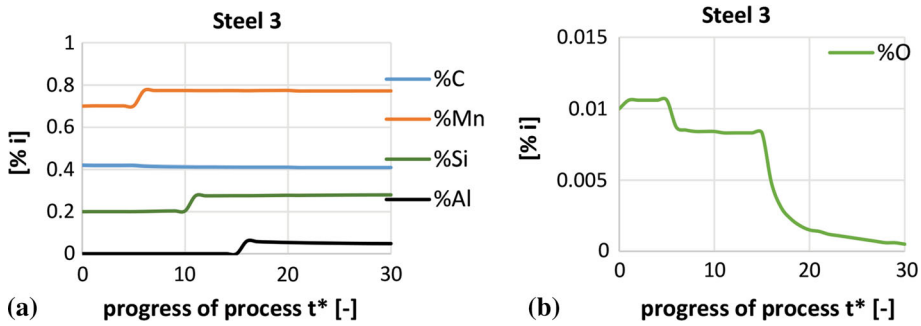

Fig. 5 Change in the chemical composition of steel 3 as a result of dosing alloy additions

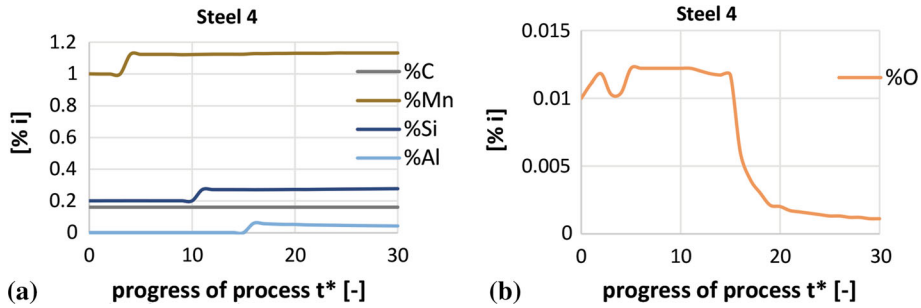

Fig. 7 Change in the chemical composition of steel 4 as a result of dosing alloy additions

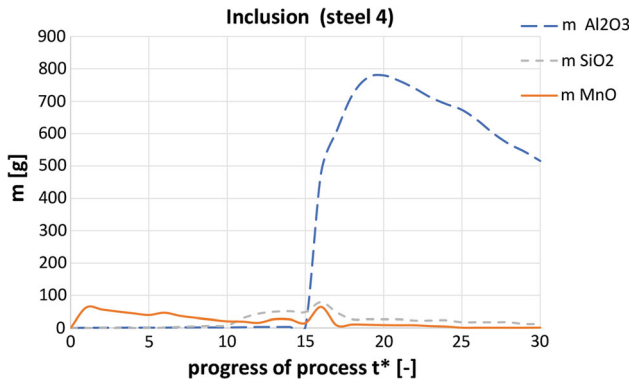

Fig. 8 Chemical composition of nonmetallic inclusions as a result of dosing alloy additions to steel 4

of 1.2% for a temperature of 1600 °C the equilibrium oxygen concentration in steel was 0.02%, assuming that the reaction resulted in the formation of pure liquid MnO and the Henry's law was satisfied. At the same assumption as for Mn, the equilibrium value of oxygen concentration of Si is obtained for the content of 0.2%Si and the temperature of 1600 °C, the equilibrium oxygen concentration in steel was 0.0324%. At the same assumptions, for the Al concentration 0.02% by mass the equilibrium oxygen concentration is $3.975 \cdot 10^{-4}$% by mass.

6. Steel Refining in Industrial Conditions

In the process conditions considered, the deoxidizing process has two stages: a) initial deoxidizing —during steel tapping from the EAF to the steelmaking ladle, and b) final deoxidizing—during refining in the ladle on an LF. Generally, Al, FeSi and FeSiMn cones are applied for the initial deoxidizing, and their amounts depend on the oxidization degree of the melt in the electric furnace.

To verify the theoretical calculations, steel samples were taken for analyzing, including chemical composition of nonmetallic inclusions (EDS) and their morphology. They were taken after refining in the LF furnace (secondary deoxidizing)—before the vacuum process.

Microstructure examinations were carried out to identify the actual chemical composition and the size of nonmetallic inclusions formed as a result of the deoxidizing process with alloy additions. They were conducted with scanning microscopy and x-ray microanalysis. Apart from the chemical analysis of nonmetallic inclusions, an attempt to assess their distribution in samples analyzed was also made. Figure 9 and 10 concerns the microstructure of steel 1, and the subsequent pictures concern steel 2. They contain an image of the microstructure and the result of x-ray microanalysis of the selected areas of precipitates.

In the sample tested—Spot 1 (Fig. 9), a cluster of fine, irregular inclusions was found, and the quantitative result indicates that Al and O are main components, indicating the presence of Al_2O_3. Figure 10 presents the microstructure of steel 1 in sample 2 (Spot 2).

In the marked area (Spot 2), the presence of S, Mn and Fe was identified, which suggests that the occurred inclusions were sulfides MnS and FeS. In performed calculations, the possibility of the formation of sulfides and oxysulfide spinels was not included, which was a consequence of the model assumptions.

The obtained results suggest that the model should be modified by additional sulfide and oxysulfide systems. However, the approach to solving these complex phase systems is problematic. Thus, the obtained EDS test results suggest that the direction of future research is correct.

A complex cluster of inclusions was identified in the microstructure image in Fig. 11 (Spot 1), and the x-ray microanalysis result shown in the table on the side confirms the presence of mainly Al and O, which suggests that the agglomerate seen at Spot 1 consists of aluminum oxide.

The chemical composition, size and distribution of inclusions within the sample volume is depend on concentrations of reacting substrate precipitates a specific inclusion. The size of inclusions is related to nucleation conditions, and stirring conditions, which favor agglomeration; thus, Al_2O_3 prevails in the composition of inclusions. However, no MnO and SiO_2 inclusions were identified in the samples tested. It can be caused by formation and floating, followed by discharging these inclusions to the slag at an early stage of refining. Also the simulation results indicate that in the steel samples taken after deoxidation, these inclusions constitute trace quantities, which can also be the reason for a lack of them in the samples tested.

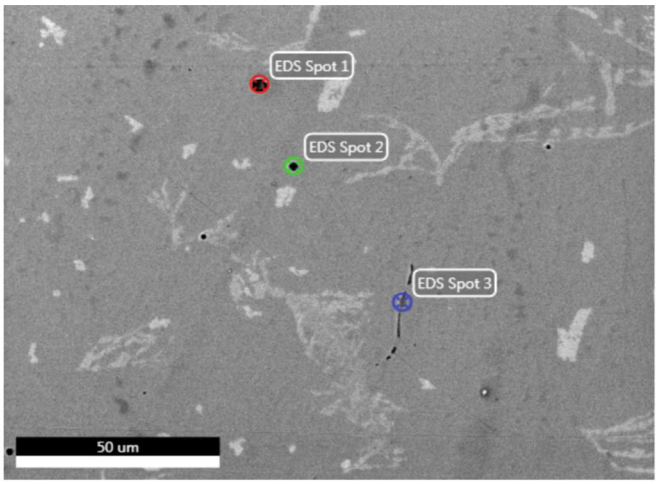

Spot 1

Element	Weight %	Atomic %
O K	43.1	60.8
MgK	3.0	2.8
AlK	30.4	25.5
S K	2.0	1.4
CaK	5.0	2.8
MnK	1.3	0.5
FeK	15.3	6.2

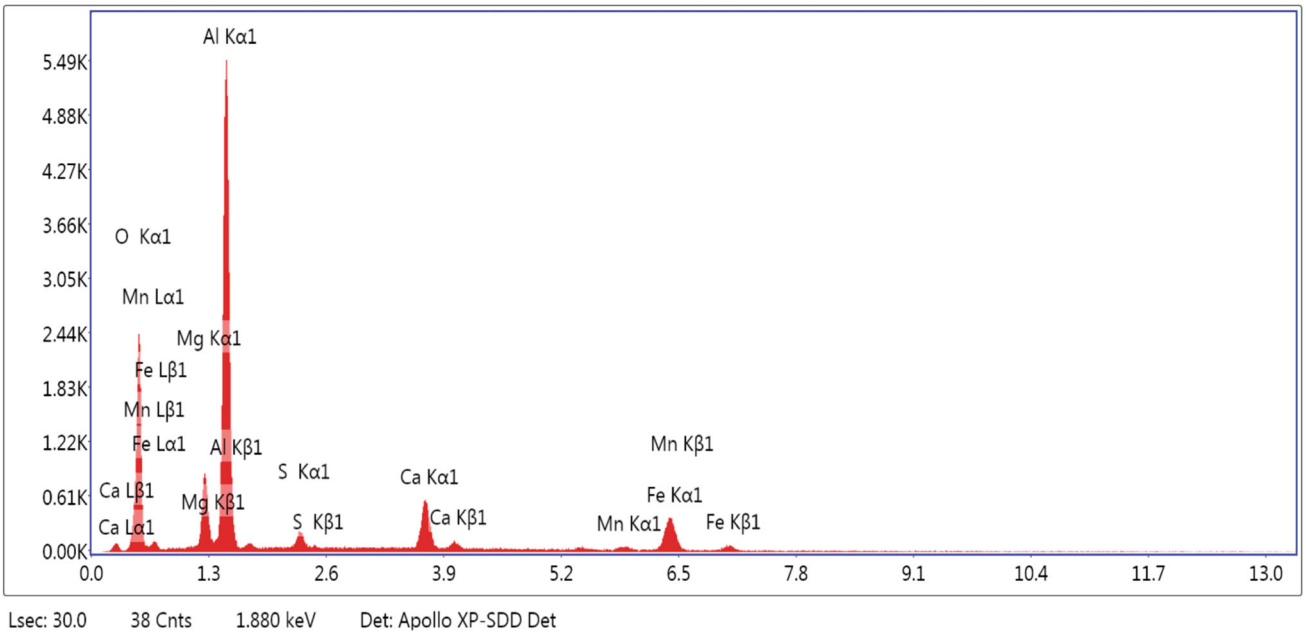

Fig. 9 Microstructure obtained in a scanning electron microscope from steel 1—sample 1. The graph of spot x-ray microanalysis from a precipitate area (Spot 1) and the result of quantitative analysis in the table

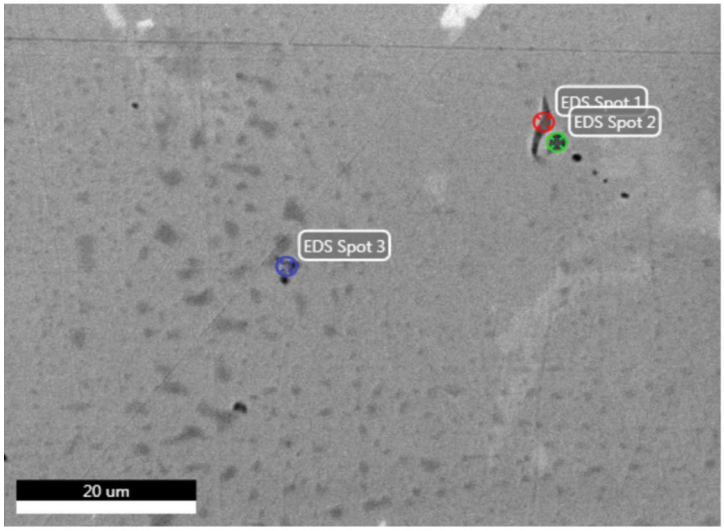

Spot 2

Element	Weight %	Atomic %
S K	26.1	37.8
CrK	4.3	3.9
MnK	32.4	27.4
FeK	37.2	31.0

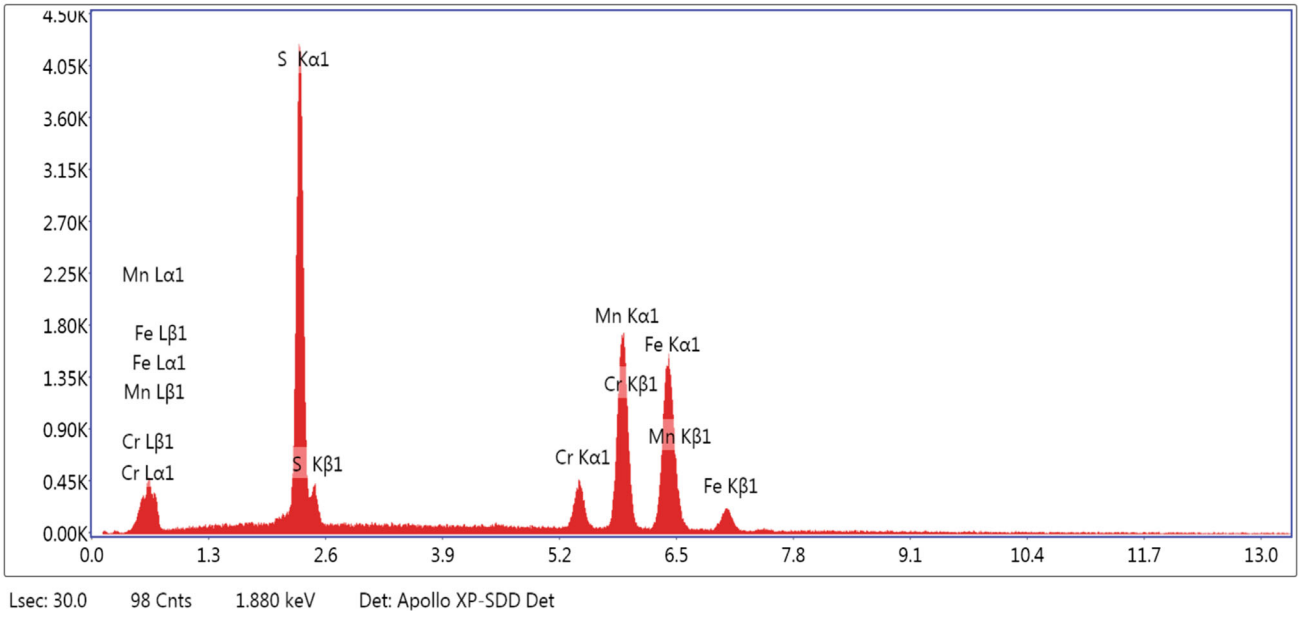

Fig. 10 Microstructure obtained in a scanning electron microscope from steel 1—sample 2. The graph of spot x-ray microanalysis from a precipitate area (Spot 2) and the result of quantitative analysis in the table

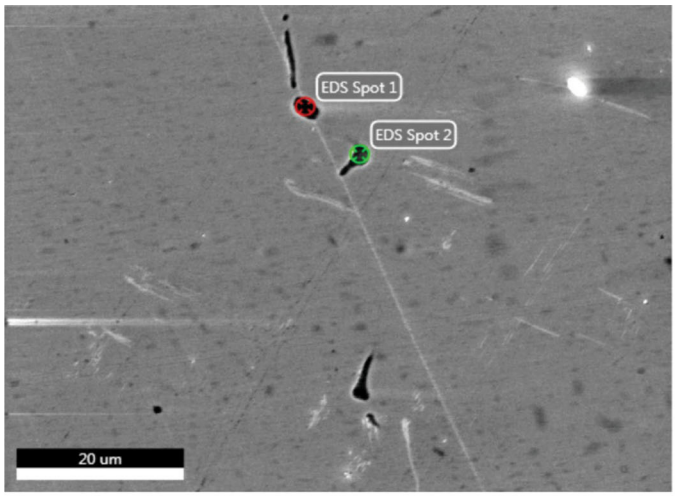

Spot 1

Element	Weight %	Atomic %
O K	9.6	24.7
MgK	0.8	1.3
AlK	9.4	14.4
S K	0.5	0.6
CrK	0.6	0.5
MnK	1.0	0.8
FeK	78.0	57.7

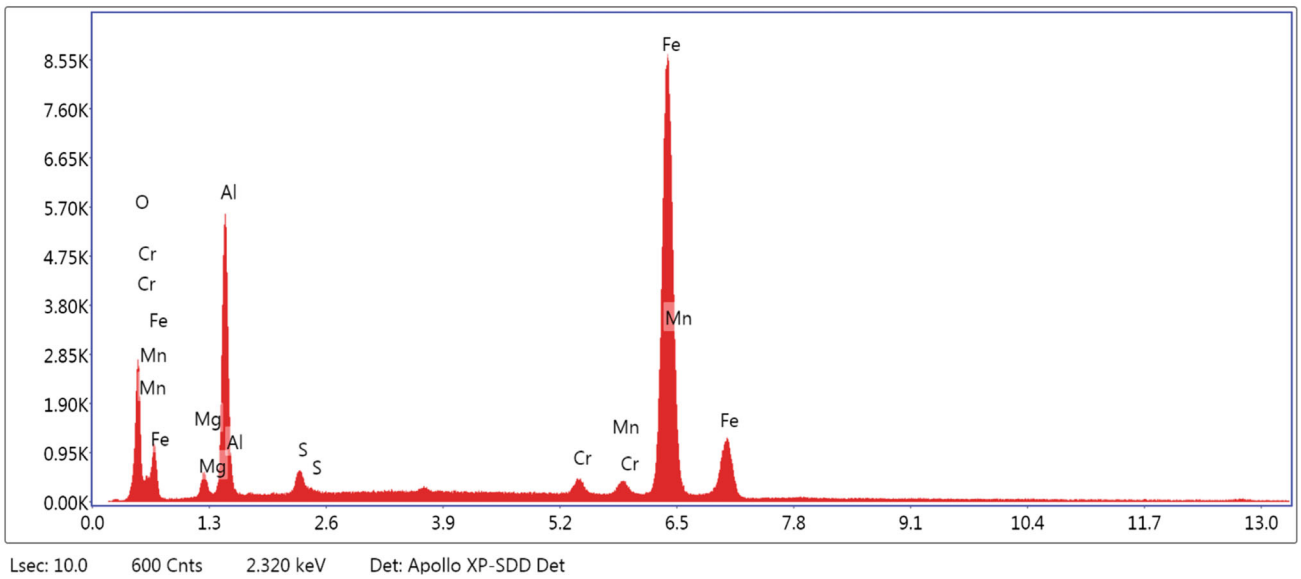

Fig. 11 Microstructure obtained in a scanning electron microscope from steel 2. The graph of spot x-ray microanalysis from a precipitate area (Spot 1) and the result of quantitative analysis in the table

7. Conclusions

Simulation of the liquid steel refining process is based upon a determination of the thermodynamic equilibrium state in the system concerned. The oxide phase composition computed above concerns a liquid solution of $MnO\text{-}SiO_2\text{-}Al_2O_3$, and for a solid solution, if occurring, it can only be indicative, as the proposed model does not include a case like this. It is related to the fact that no data are available, which would enable the solid solution component activities to be presented.

In the steel samples tested, taken after ladle deoxidizing, mainly oxide inclusions of type Al_2O_3 were identified. Also the sulfur-based inclusions MnS and FeS were found. The proposed solution and the results of simulation of the ladle steel refining process do not include the formation of sulfides, e.g., MnS or FeS, and oxysulfides, whose presence could be

identified in the steel samples taken from heats. The adopted assumptions on the order of alloy addition introduction confirm the effectiveness of the refining carried out and accurately visualize the occurring processes. The obtained results reflect the process well, which allows us to suppose that after updating the database with data on sulfides and oxysulfides, it will be possible to simulate the ladle steel refining process accurately.

Acknowledgments

The research was conducted with the financial support as part of the Project: No. POIR.01.02.00–00-0207/17, title: ''Innovative manufacturing process for a very high metallurgical purity steel for the most critical applications in the automotive industry''.

References

1. A. Pribulova, J. Babic, and D. Baricova, Influence of Hadfields Steel Chemical Composition on this Mechanical Properties. *Chem. List.* **105**(4), 430–432 (2011)
2. D. Kalisz, S. Gerasin, P. Bobrowski, P.L. Żak, and T. Skowronek, Computer Simulation of Microsegregation of Sulphur and Manganese and Formation of MnS Inclusion While Casting Rail Steel. *Arch. Metall. Mater.* **61**(4), 1939–1944 (2016)
3. C.D. Liu, M.N. Bassim, and S. St. Lawrence, Evaluation of Fatigue-crack Initiation at Inclusions in Fully Pearlitic Steels. *Mat. Sci. Eng. A* **167**(1–2), 107–113 (1993)
4. T. Miyake, M. Morishita, H. Nakata, and M. Kokita, Influence of Sulphur Content and Molten Steel Flow on Entrapment of Bubbles to Solid/Liquid Interface. *ISIJ Int.* **46**, 1817–1822 (2006)
5. B. Bulko, M. Molnar, P. Demeter, D. Baricova, A. Pribulova, and P. Futas, Study of the Influence of Intermix Conditions on Steel Cleanliness. *Metals* **8**(10), 852–861 (2018)
6. J. Iwanciw, D. Podorska, and J. Wypartowicz, Simulation of Oxygen and Nitrogen Removal from Steel by Means Titanium and Aluminium. *Arch. Metall. Mater.* **53**(3), 635–644 (2011)
7. D. Podorska, P. Drożdż, J. Falkus, and J. Wypartowicz, Calculation of Oxide Inclusion Composition in the Steel Deoxidized with Mn Si, and Ti. *Arch. Metall. Mater.* **51**(4), 581–586 (2006)
8. T. Lipiński, and A. Wach, Non-metallic Inclusion Structure Dimension in High Quality Steel with Medium Carbon Contents. *Arch. Found. Eng.* **9**(3), 75–78 (2009)
9. H.V. Atkinson, and G. Shi, Characterization of Inclusions in Clean Steels: A Review Including the Statistics of Extremes Methods. *Prog. Mater. Sci.* **48**(5), 457–520 (2003)
10. I.H. Jung, Y.B. Kang, S.A. Decterov, and A.D. Pelton, Thermodynamic Evaluation and Optimization of the MnO-Al_2O_3 and MnO-Al_2O_3-SiO_2 Systems and Applications to Inclusion Engineering. *Metall. Mater. Trans. B* **35B**, 259–268 (2004)
11. J. Iwanciw, D. Podorska, and J. Wypartowicz, Modeling of Oxide Precipitates Chemical Composition during Steel Deoxidization. *Arch. Metall. Mater.* **56**(4), 999–1005 (2011)
12. D. Kalisz: *Termodynamiczna Charakterystyka Powstawania Fazy Niemetalicznej w Ciekłej stali*, 1st ed. (Wydawnictwo naukowe Akapit, Kraków, 2013), pp. 5–193 (**in Polish**)
13. H. Ohta, and H. Suito, Activities in MnO-SiO_2-Al_2O_3 Slags and Deoxidation Equilibria of Mn and Si. *Met. Mater. Trans. B* **27B**, 263–270 (1996)
14. K. Tomioka, K. Ogawa, and H. Matsumoto: Thermodynamics of Reaction between Trace Amount of Al. and Inclusion in Mn-Si Killed Steel. *ISIJ Int.* **36**, 101–104 (1996)
15. S. Kobayashi, Thermodynamic Fundamentals for Alumina-Content Control of Oxide Inclusions in Mn-Si Deoxidation of Molten Steel. *ISIJ Int.* **39**, 664–670 (1999)
16. V.Y. Dashevskii, A.M. Katsnelson, N.N. Makarova, K.V. Grigorovitch, and V.I. Kashin, Deoxidation Equilibrium of Manganese and Silicon in Liquid Iron-Nickel Alloys. *ISIJ Int.* **43**, 1487–1494 (2003)
17. Z. Liu, J. Wei, and K. Cai, A Coupled Mathematical Model of Microsegregation and Inclusion Precipitation during Solidification of Silicon Steel Alloys. *ISIJ Int.* **42**, 958–963 (2002)
18. N. Tanahashi, C. Furuta, and T. Yamauchi, Fujisawa: Phase Equilibria of the MnO-SiO_2-CrOx System at 1873 K under Controlled Oxygen Partial Pressure. *ISIJ Int.* **41**, 1309–1315 (2001)
19. E. T. Turkdogan: *Physicochemical Properties of Molten Slags and Glasses*, 1st ed. (The Metals Society, London 1983), pp. 5–530
20. S. Ban-ya, Mathematical Expressions of Slag-Metal Reactions in Steelmaking Process by Quadratic Formalism Based on the Regular Solution Model. *ISIJ Int.* **33**, 2–11 (1993)
21. J. Iwanciw, The Coefficients of Regular Solution Model for Steelmaking Slags. *Arch. Met. Mater.* **49**, 595–609 (2004)